Application Note

Cell Analysis

Agilent

Trusted Answers

Optimized High-Throughput 3D Cell Culture Assays with Kinetic Imaging and Endpoint Viability Analysis

Image- and luminescence-based viability quantification for scalable treatment-response characterization of 3D cell culture models

Authors

Ernest Heimsath, PhD,
Joe Clayton, PhD,
Agilent Technologies, Inc.

Abstract

Three-dimensional (3D) cell culture models are increasingly used in drug discovery and new approach methodology (NAM)-based workflows because they more closely replicate physiologically relevant tissue characteristics. Effective implementation of these models requires scalable methods for evaluating formation, quality, and treatment response.

This application note demonstrates an imaging-centered workflow using an HT-1080 spheroid model. Automated brightfield and fluorescence imaging on the Agilent BioTek Cytation 9 cell imaging multimode reader was used to monitor 3D model formation, quantify size and uniformity, and measure treatment-induced cytotoxicity over time using Agilent eTox Red stain as a representative fluorescent cell death marker. An orthogonal Promega CellTiter-Glo 3D Cell Viability Assay was subsequently performed to provide endpoint ATP-based viability confirmation.

Together, kinetic imaging and endpoint viability measurements provide complementary information linking model quality, response kinetics, and treatment outcome, supporting scalable characterization and optimization of 3D cell culture models for NAM-relevant assay development.

Introduction

3D cell culture models, including spheroids and organoids, more closely replicate tissue architecture, cell-cell interactions, and microenvironmental complexity than conventional two-dimensional cultures. As a result, they are increasingly used in oncology research, disease modeling, and drug discovery to improve the physiological relevance of in vitro studies.[1–6] These systems also support the broader adoption of NAMs, which aim to improve predictive biology while reducing dependence on animal testing.[7]

Despite their advantages, implementing 3D culture models in scalable screening workflows remains challenging. Generation and maintenance of reproducible spheroids can be labor-intensive, while studies of growth, maturation, and treatment response often require measurements collected across multiple time points. In addition, imaging and quantitative analysis of 3D models can present challenges related to focus, contrast, segmentation, and consistency between wells. These factors can limit throughput and complicate assay optimization without robust acquisition and analysis workflows.

Automated imaging approaches help address these challenges by enabling kinetic brightfield and fluorescence-based monitoring of 3D culture formation, morphology, viability, and treatment response. Combined with quantitative image analysis, these workflows support measurements of spheroid size, uniformity, circularity, compaction, and fluorescence intensity. When integrated with automated incubation and plate handling, they provide a scalable framework for long-term experiments with improved reproducibility and reduced manual intervention.

The Cytation 9 cell imaging multimode reader integrates automated imaging, multimode detection, and quantitative analysis within a single platform. In this application note, Cytation 9 was used to address three analytical objectives. First, kinetic, brightfield, and fluorescence imaging was used to monitor 3D model formation and assess characteristics that support assay optimization, including size, uniformity, and compaction. Second, automated fluorescence imaging was used to quantify treatment-induced cytotoxicity with an Agilent eTox Red stain as a representative cell death marker. Finally, an orthogonal CellTiter-Glo 3D Cell Viability Assay was performed to measure ATP as an endpoint indicator of metabolically active cells. Together, these approaches demonstrate how kinetic imaging and endpoint viability measurements can be combined to characterize 3D cell culture models, improve assay development, and support NAM-relevant research workflows. Figure 1 provides an overview of the integrated workflow, from 3D mode l formation and kinetic imaging-based characterization through treatment-response monitoring and endpoint viability confirmation.

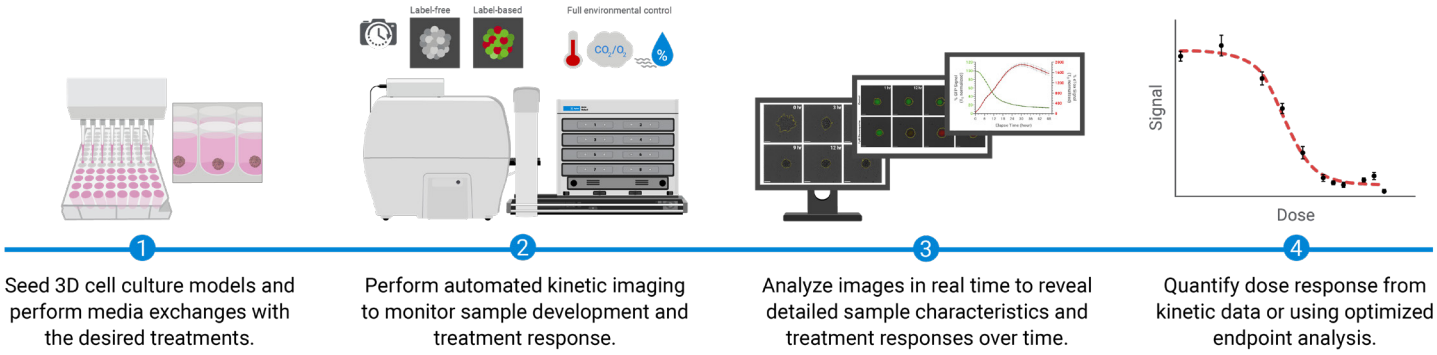

Figure 1. Workflow for kinetic imaging and analysis of 3D cell culture models. Samples are seeded and treated, monitored using automated kinetic imaging under environmental control, analyzed in real time, and quantified using kinetic and endpoint dose-response measurements..

Experimental

Cell line

HT-1080 fibrosarcoma cells (part number CCL-121) were purchased from ATCC (Manassas, VA, USA). A derivative cell line stably expressing a nuclear-localized GFP fluorescent protein (HT-1080-NLS-GFP) was generated using Agilent eLenti-Green (part number 8711010) according to the manufacturer's guidelines.

3D model formation

Adherent HT-1080 cell cultures were detached using TrypLE Express (part number 12605036; Thermo Fisher Scientific; Waltham, MA, USA), pelleted by centrifugation at 300 G, then resuspended in 1x DPBS. Cells were reseeded in Nunclon Sphera 96-Well, Nunclon Sphera-Treated, U-Shaped-Bottom Microplates (part number 174929; Thermo Fisher Scientific) at a density of 2×10^3 cells/well and monitored during spheroid formation. This representative spheroid workflow was used to demonstrate kinetic imaging-based assessment of 3D cell culture formation, including measurements of size, uniformity, compaction, and related attributes that can be used to optimize assay timing and model quality before treatment studies.

Drug treatment

Fully formed spheroids were transferred to Corning 96-well Round Bottom Ultra-Low Attachment Surface Spheroid Microplates (product number 4520), which have an 87.5 µm thick well bottom that is ideal for imaging assays. Wells were prefilled with media containing 250 nM Agilent eTox Red stain (part number 8711009) and variable concentrations of staurosporine (product number 1285; Tocris Biosciences). eTox Red was selected as the demonstrated fluorescent cytotoxicity reagent for this workflow, but the acquisition and analysis strategy is intended to be adaptable to other compatible fluorescent markers of viability, cell death, or related cell health endpoints.

Image acquisition

Image acquisition was organized to support two stages of 3D cell culture characterization. For kinetic monitoring of 3D model formation, images were acquired using both label-free brightfield imaging and fluorescent imaging of the HT-1080-NLS-GFP model. Brightfield imaging provided a reagent-free method to assess spheroid formation, size, morphology, and compaction over time, while GFP fluorescence provided a label-based method for defining the spheroid and comparing formation attributes across wells. For treatment-response studies, GFP and CY5 fluorescence channels were acquired to monitor the spheroid and eTox Red staining, respectively. This demonstrated channel configuration reflects the selected GFP spheroid label and eTox Red cytotoxicity reagent; other fluorescent viability or cell health markers could be incorporated by selecting compatible excitation and emission channels and adapting the analysis workflow accordingly. Imaging was performed using the Cytation 9 cell imaging multimode reader equipped with a 10x 0.3 NA objective. Kinetic imaging was accomplished by coupling Cytation 9 with an Agilent BioTek BioSpa 8 automated incubator, enabling scheduled incubation and automated plate handling for multiple-time-point imaging. Laser autofocus was employed for rapid focusing on each well to support reproducible image acquisition across the time course.

Image analysis

Image and plate reader-based analysis were performed to quantify three primary categories of 3D cell culture characteristics. First, formation kinetics and model quality were evaluated from both brightfield and fluorescent images. Brightfield-based segmentation was used to quantify morphology-based attributes such as projected area, diameter, circularity, compaction, and well-to-well uniformity over time. Fluorescence-based segmentation of GFP-positive spheroids provided an alternative label-based measurement of spheroid size and uniformity, with improved contrast for spheroid identification in the representative HT-1080-NLS-GFP model. Second, treatment-induced cytotoxicity was quantified from eTox Red fluorescence as the demonstrated fluorescent cell death marker. Fluorescence images were preprocessed for background subtraction, followed by independent Cellular Analysis steps for GFP and eTox Red signals. eTox Red fluorescence was used as the kinetic cell death readout and was adjusted using the initial spheroid area based on GFP signal. The area-corrected eTox Red signal was then normalized to fold-change relative to control at each respective time point. Third, endpoint luminescence data from the CellTiter-Glo 3D Assay were analyzed as a bulk ATP-based viability readout. These endpoint results were interpreted alongside the kinetic imaging data so that final viability measurements could be linked to model formation quality, initial spheroid size, uniformity, and the time-resolved trajectory of treatment response.

Endpoint plate reader viability assay

Following kinetic imaging, induced cytotoxicity was also evaluated using an orthogonal endpoint plate reader-based assay. The CellTiter-Glo 3D Assay was used to measure ATP as a luminescent indicator of metabolically active cells in treated 3D cultures. This endpoint measurement was performed after the imaging time course, allowing the final viability readout to be interpreted in the context of the preceding kinetic imaging data, including spheroid formation quality, initial size and uniformity, timing of response onset, and treatment-dependent changes in morphology or fluorescent cytotoxicity signal.

Results and discussion

Kinetic monitoring of 3D cell culture formation for assay optimization

Brightfield imaging approach

Label-free brightfield imaging was used to monitor 3D cell culture formation kinetically and quantify morphology-based attributes relevant to assay optimization (Figure 2). In the representative HT-1080 spheroid workflow, dispersed cells initially occupied a relatively large projected area at the bottom of the well (Figure 2A). As cells coalesced and compacted, the brightfield-derived area decreased and then stabilized, indicating formation of a mature spheroid suitable for downstream assays. Associated brightfield images and graphs show changes in size, morphology, compaction, and well-to-well uniformity over time (Figure 2B). These measurements provide a practical quality-control step for identifying wells or conditions that meet assay-readiness criteria before treatment. The primary strength of this approach is that it is noninvasive and reagent-free, reducing assay complexity and preserving fluorescence channels for other measurements. Its main limitation is that it primarily reports morphology; by itself, it does not directly distinguish viable from nonviable cells or identify specific molecular or cellular phenotypes.

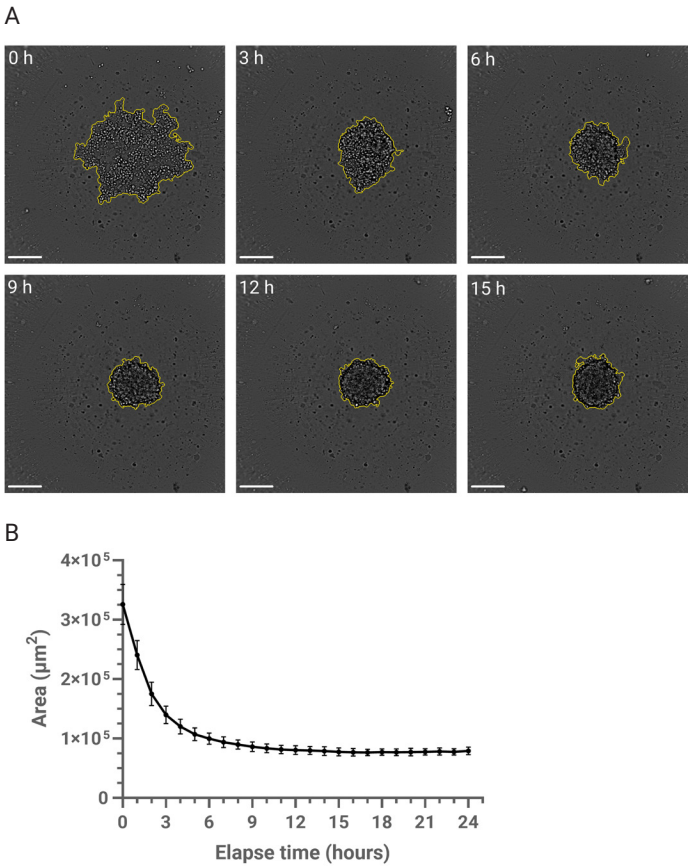

Figure 2. Label-free kinetic monitoring of 3D cell culture models. (A) Time lapse of spheroid formation of HT-1080 cells that are sedimented in the bottom of a 96-well U-bottom microplate. Scale bar = 200 µm. (B) Quantification of spheroid area based on brightfield signal. Area (µm^2) and error bars (standard deviation) are derived from all spheroids across a full 96-well microplate (n = 96).

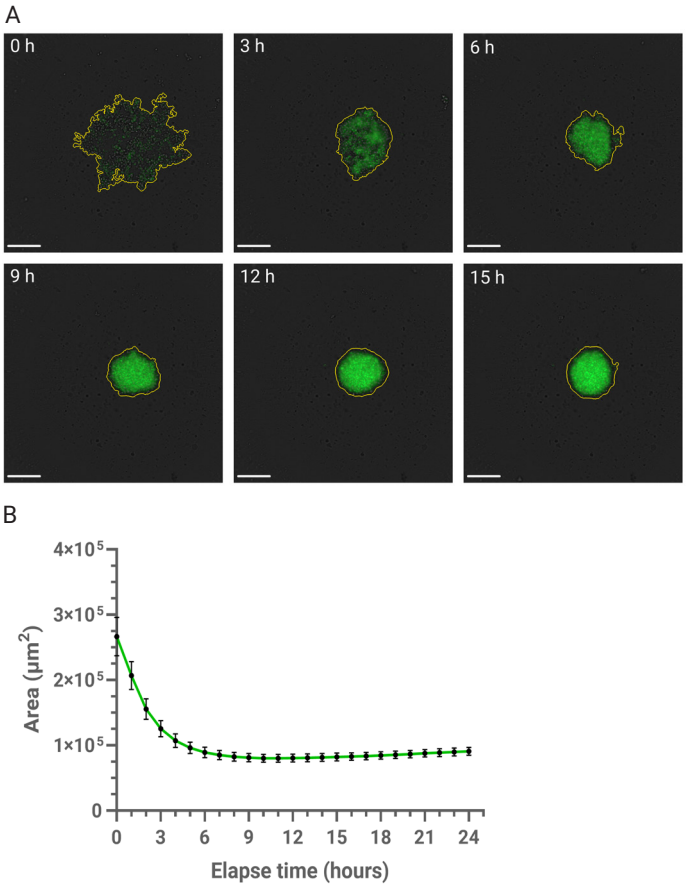

Figure 3. Fluorescence-based kinetic monitoring of 3D cell culture models. (A) Time lapse of spheroid formation of HT-1080 cells expressing nuclear-localized GFP that are sedimented in the bottom of a 96-well U-bottom microplate. Scale bar = 200 µm. (B) Quantification of spheroid area based on GFP fluorescence signal. Mean area (µm^2) and error bars (standard deviation) are derived from all spheroids across a full 96-well microplate (n = 96).

Label-based fluorescence imaging approach

Label-based fluorescence imaging provided a complementary method for quantifying 3D model formation and uniformity (Figure 3). In the HT-1080-NLS-GFP model, nuclear-localized GFP enabled fluorescence-based identification of the spheroid, supporting measurements of the spheroid area, size distribution, and well-to-well consistency during formation (Figure 3B). This approach can improve object definition when brightfield contrast is limited and can support more consistent segmentation of spheroids in automated analysis workflows. As a result, fluorescent spheroid labeling can be useful for plate-level statistics, replicate comparison, and confirmation that model formation is sufficiently reproducible for downstream treatment studies. Its primary strength is improved contrast and measurement specificity for labeled spheroids. Its limitations are that it requires a compatible fluorescent label or engineered cell model, may not be suitable for all 3D culture systems, and uses fluorescence channels that may otherwise be reserved for functional readouts.

Fluorescent label-based quantification of treatment-induced cytotoxicity and viability response

After formation conditions were established, automated kinetic fluorescence imaging was used to quantify treatment-induced cytotoxicity. Fully formed HT-1080 spheroids were treated with staurosporine in the presence of eTox Red stain, which selectively labels nuclei in cells with compromised membrane integrity, indicating cell death. Staurosporine treatment produced a concentration-dependent decrease in endogenous GFP signal (Figures 4A and B) with an EC_{50} at 24 hours of 2.7 nM (Figure 4C). Conversely, staurosporine treatment produced a concentration-dependent increase in eTox Red signal (Figure 5).

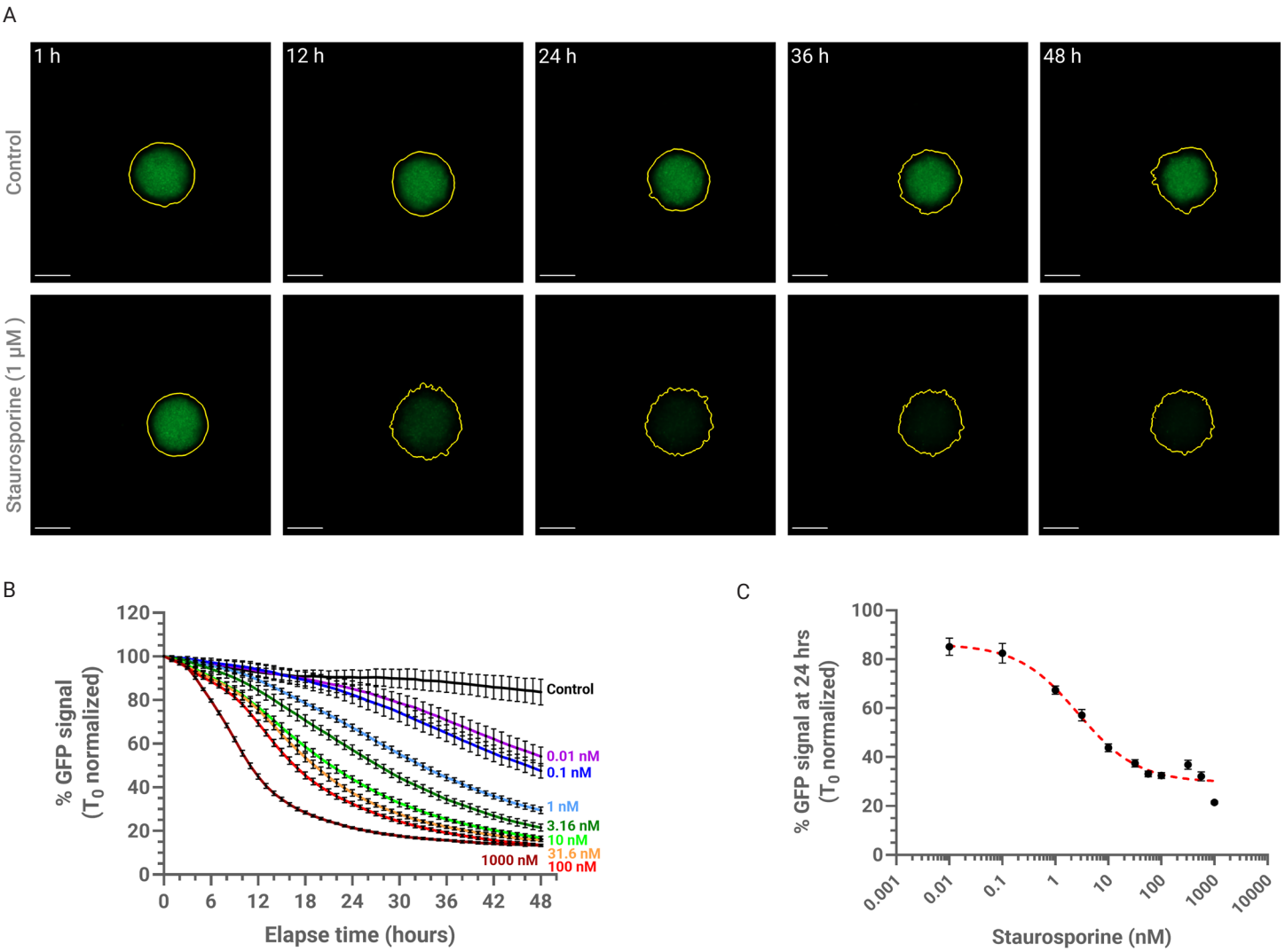

Figure 4. Kinetic quantification of drug-induced toxicity using endogenously expressed GFP. (A) Time lapse of HT-1080-NLS-GFP spheroids treated with vehicle control (top row) or 1 µM staurosporine (bottom row). Scale bar = 200 µm. GFP fluorescence is retained in control, while it is lost when spheroids are exposed to staurosporine. Scale bar = 200 µm. (B) Segmented masks of fluorescent signal based on (A) (yellow outline) were used to quantify endogenous GFP signal induced by staurosporine, indicating that it is dose-dependent (B) with an EC_{50} of 2.7 nM by 24 hours (C).

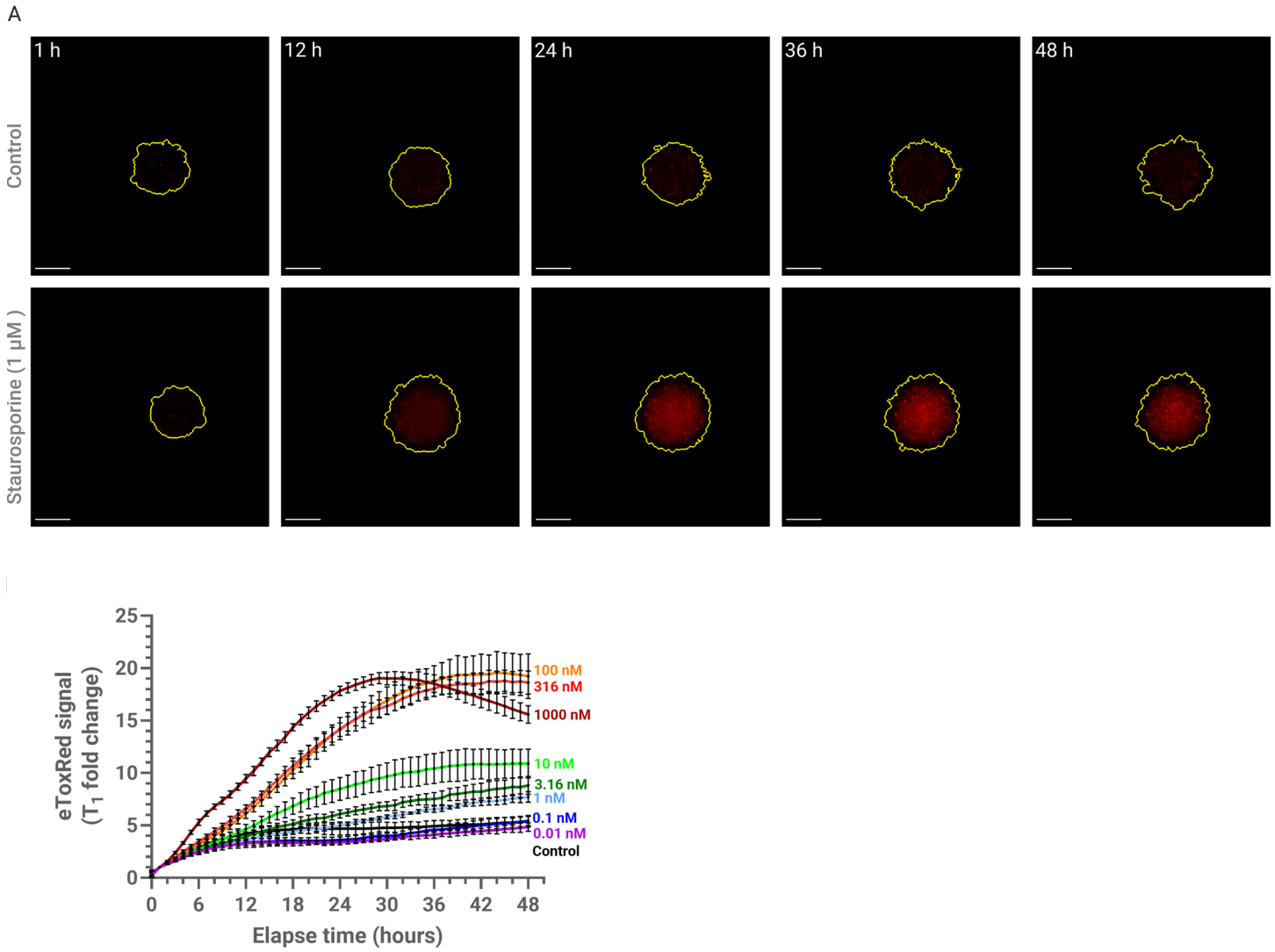

Figure 5. Kinetic quantification of drug-induced toxicity using eTox Red, a live toxicity fluorescent dye. (A) Time lapse of HT-1080-NLS-GFP spheroids treated with vehicle control (top row) or 1 µM staurosporine (bottom row). eTox Red signal remains basal in control relative to spheroids treated with 1 µM staurosporine. Scale bar = 200 µm. (B) Segmented masks of fluorescent signal based on (A) (yellow outline) were used to quantify eTox Red signal induced by staurosporine, indicating that it is dose-dependent (B).

As demonstrated, staurosporine treatment induces an inverse trend in kinetic GFP signal compared to eTox Red signal (Figure 6). The relationship between the two fluorescent indicators can be expressed as a ratio (eTox Red:GFP) and is termed here as the Toxicity Index.

Similar to the eTox Red signal, the staurosporine treatment produced a concentration-dependent increase in Toxicity Index (Figure 7A), with an EC_{50} of 20.9 nM (Figure 7B).

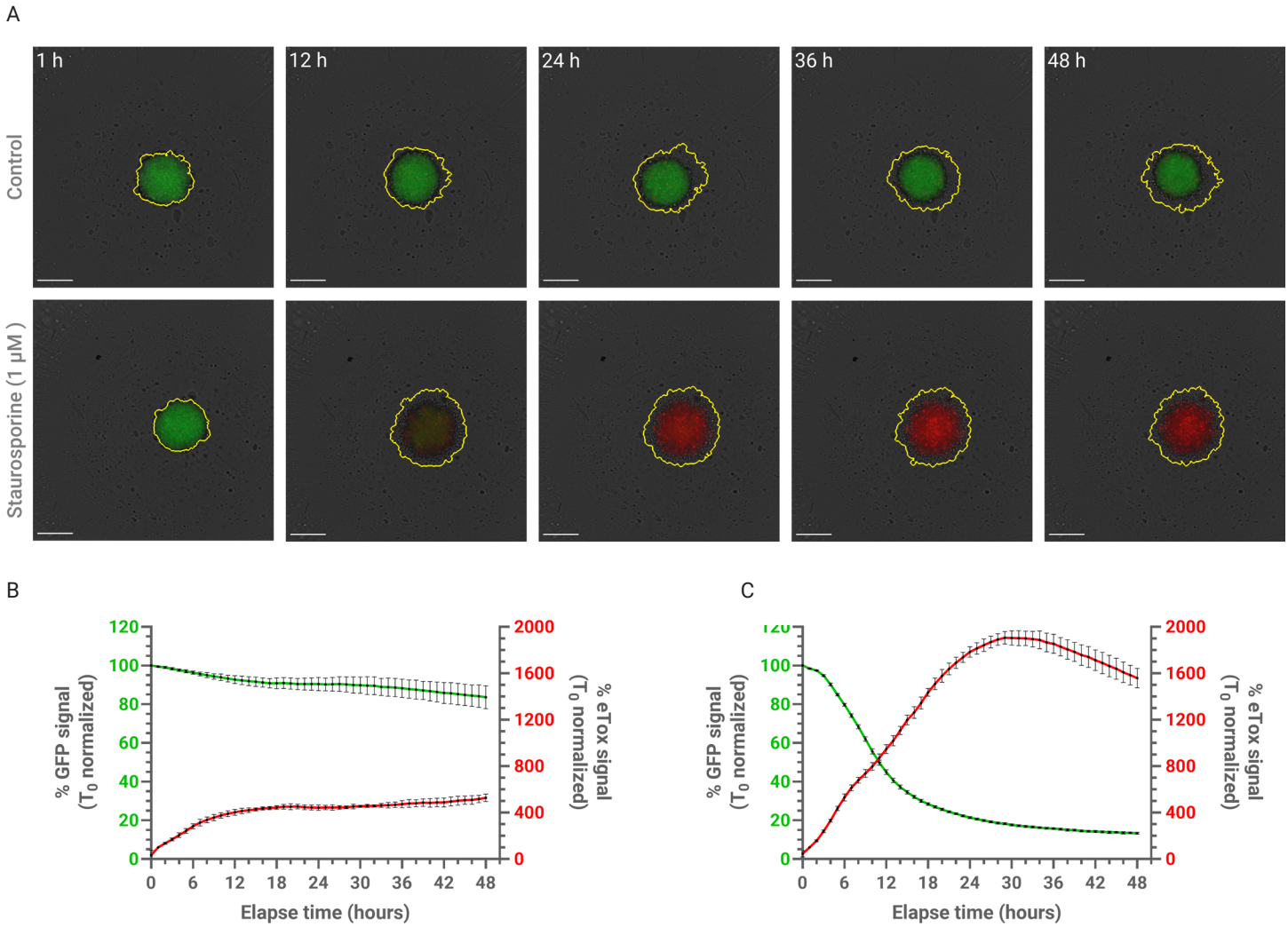

Figure 6. Comparison of kinetic response profiles for endogenously expressed signal and toxicity dye. (A) Time-lapse images of HT-1080-NLS-GFP spheroids showing endogenous GFP signal (green) overlaid with eTox Red signal (red) in control treatment (top row) or in the presence of 1 µM staurosporine (bottom row). Scale bar = 200 µm. Quantification of both kinetic signal profiles is indicated for control (B) or with 1 µM staurosporine (C) indicate an inverse kinetic relationship between endogenous "viability" GFP signal and eTox Red toxicity signal in response to drug treatment.

This approach provides a quantitative, time-resolved readout that can be normalized to initial spheroids size and adapted to different fluorescent markers depending on the biological question, such as membrane integrity, live-cell signal, apoptosis, metabolic activity, or other viability-associated endpoints. Its limitations are marker-specific: fluorescent reagent addition may introduce assay-dependent constraints, and results may be influenced by dye penetration, optical attenuation, compound fluorescence, marker mechanism, or treatment responses that are not captured by the selected endpoint. While demonstrated using HT-1080 spheroids and eTox Red, this workflow is broadly applicable to 3D cell culture models and spheroids when compatible fluorescence-based viability, cytotoxicity, or cell health readouts are incorporated. This generality is important for NAM-focused workflows because the same analytical framework can support model qualification, treatment-response characterization, and comparison of biologically relevant assay conditions without requiring a single fixed reagent or endpoint.

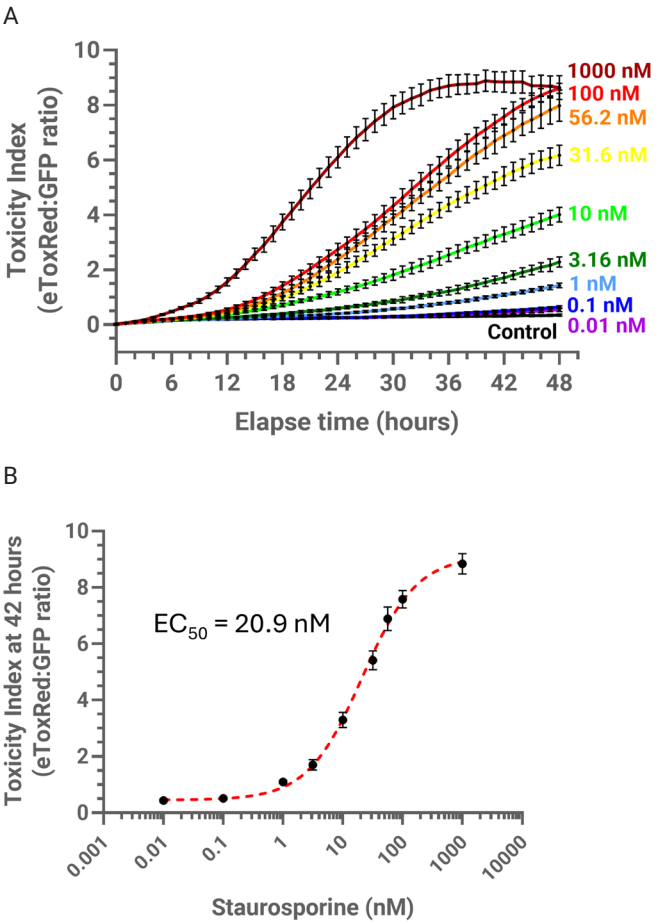

Figure 7. The Toxicity Index describes the relationship between viability (GFP) and toxicity (eTox Red) signals. (A) Kinetic profile of the ratio of eToxRed signal to endogenous GFP signal (Toxicity Index) in HT-1080-GFP spheroids in the presence of increasing concentration of staurosporine. (B) Quantification of staurosprine dose response at 24 hours based on Toxicity Index with an EC_{50} of 20.9 nM.

Orthogonal endpoint plate reader-based quantification using CellTiter-Glo 3D

To complement the kinetic imaging workflow, an orthogonal endpoint viability assay was performed at the 24-hour time point using the CellTiter-Glo 3D Assay (Figure 8). This assay measures ATP as a luminescent indicator of metabolically active cells and is optimized for use with 3D culture models. Staurosporine treatment produced a concentration-dependent reduction in ATP signal with an IC_{50} of 3.8 nM, consistent with the cytotoxic effects observed in fluorescence imaging.

The primary strength of the CellTiter-Glo 3D Assay is its ability to provide a sensitive, scalable, and straightforward measure of overall viability that is well suited for screening applications. As a bulk endpoint measurement, however, it does not provide information regarding morphology, spatial distribution of signal, or the timing of treatment response. Consequently, ATP-based viability measurements are most informative when interpreted alongside additional information regarding model quality and treatment-associated changes.

This demonstrated workflow highlights the use of the CellTiter-Glo 3D Assay as an orthogonal endpoint viability assay for confirming treatment effects in 3D cell culture models.

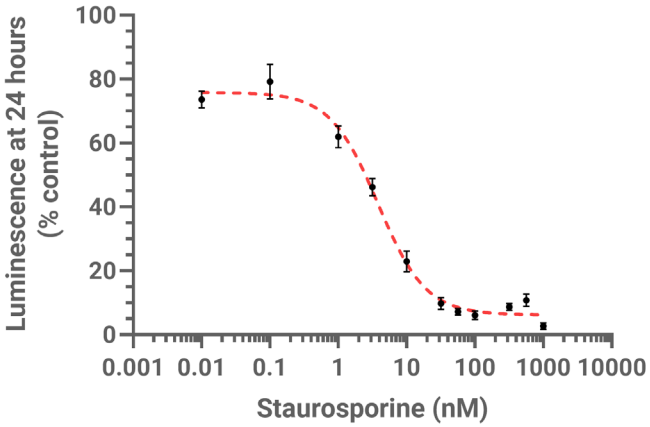

Figure 8. Quantification of drug response in a 3D cell culture model using CellTiter-Glo 3D Assay. Quantification of CellTiter-Glo 3D luminescence of HT-1080-GFP spheroids after a 24-hour exposure to increasing concentration of staurosporine with an IC_{50} of 3.8 nM.

Conclusions

This work demonstrates an imaging-centered workflow for the characterization and optimization of 3D cell culture models using the Agilent BioTek Cytation 9 cell imaging multimode reader (Table 1). Kinetic, brightfield, and fluorescence imaging enabled quantitative evaluation of model formation by measuring attributes such as size, morphology, compaction, and uniformity over time, providing objective metrics to guide assay optimization and establish assay-ready conditions. In addition, kinetic fluorescence imaging supported time-resolved characterization of treatment-induced effects, enabling quantitative assessment of cytotoxicity and treatment response within the same experimental workflow.

The demonstrated CellTiter-Glo 3D Assay provided an orthogonal endpoint measure of ATP-associated viability and served as a representative example of how imaging-derived information can enhance interpretation of downstream analytical measurements. By establishing model quality before treatment and capturing the onset and progression of biological response, kinetic imaging provides critical context that is not available from endpoint measurements alone.

Together, these approaches illustrate how imaging can serve as a foundational analytical tool for 3D cell culture workflows, supporting both assay development and treatment-response characterization while informing interpretation of endpoint viability assays and other complementary analytical platforms. This integrated strategy provides a practical framework for NAM-relevant research and drug discovery applications using spheroids, organoids, and other advanced 3D cell culture models.

Table 1. Image- and luminescence-based 3D cell culture workflow approaches.

Workflow Objective	Approach	Primary Measurements	Strengths	Limitations
Kinetic Monitoring of 3D Cell Culture Formation	Label-free brightfield imaging	Projected area, diameter, morphology, compaction, and well-to-well uniformity	Noninvasive, reagent-free, simple to implement, and well suited for assay-readiness QC and optimization	Primarily morphology-based and does not directly measure viability or specific phenotypes
Kinetic Monitoring of 3D Cell Culture Formation	Fluorescent label-based imaging	Fluorescence-defined spheroid area, size distribution, and uniformity	Improved contrast and spheroid definition for automated segmentation, replicate comparison, and plate-level statistics	Requires a compatible label or engineered model and uses fluorescence channels
Treatment-Induced Cytotoxicity or Viability Response Quantification	Fluorescent label-based imaging demonstrated with Agilent eTox Red	Area-normalized fluorescent viability, cytotoxicity, or cell health signal over time	Provides a quantitative kinetic readout that can be adapted to compatible fluorescent markers and endpoint-specific assay designs	Requires marker selection and validation; may be affected by reagent penetration, optical attenuation, compound fluorescence, or endpoint-specific biological limitations
Orthogonal Endpoint Viability Confirmation	Plate reader-based CellTiter-Glo 3D luminescence assay	Endpoint ATP-based viability signal representing metabolically active cells	Simple, scalable, sensitive bulk viability readout that complements imaging-derived kinetic and morphological context	Endpoint and destructive; does not provide spatial information, morphology, or response timing

References

1. Hirschhaeuser, F.; Menne, H.; Dittfeld, C.; West, J.; Mueller-Klieser, W.; Kunz-Schughart, L. A. Multicellular Tumor Spheroids: An Underestimated Tool is Catching Up Again. *J Biotechnol* **2010**, *148*(1):3-15. DOI: doi.org/10.1016/j.jbiotec.2010.01.012
2. Nath, S.; Devi, G.R. Three-Dimensional Culture Systems in Cancer Research: Focus on Tumor Spheroids Model. *Pharmacol Ther* **2016**, 163:94–10. DOI: doi.org/10.1016/j.pharmthera.2016.03.013
3. Thoma, C. R.; Zimmermann, M.; Agarkova, I.; Kelm, J. M.; Krek, W. 3D Cell Culture Systems Modeling Tumor Growth Determinants in Cancer Target Discovery. *Adv Drug Deliv Rev* **2014**, *6*(9–70):29–41. DOI: doi.org/10.1016/j.addr.2014.03.001
4. Friedrich, J.; Seidel, C.; Ebner, R.; Kunz-Schighart, L. A. Spheroids-Based Drug Screen: Considerations and Practical Approach. *Nat Protoc* **2009**, 4:309-324. DOI: doi.org/10.1038/nprot.2008.226
5. Wang, Y.; Jeon, H. 3D Cell Cultures Toward Quantitative High-Throughput Drug Screening. *Trends Pharmacol Sci.* **2022**, *43*(7):569-581 DOI: doi.org/10.1016/j.tips.2022.03.014
6. Liang, Z.; Aslam, M.; Haq, W. U. I.; Wiesler, M.; Mutlu, S. N.; Stahlhut, P.; Verma-Fuehring, R.; Zahn, I.; Paulsen, F. P.; Groll, J. et al. A High-Throuhgput 3D Conjunctival Spheroids Model for Standardized In Vitro Testing. *Sci Reports* **2026**, *16*(23101). DOI: doi.org/10.1038/s41598-026-63887-0
7. United States Food and Drug Administration. New Approach Methodologies. New Approach Methodologies (NAMs) | FDA

Products used in this application

Agilent products

BioTek Cytation 9 Cell Imaging Multimode Reader

Other products

Promega CellTiter-Glo 3D Cell Viability Assay

www.agilent.com/lifesciences/biotek

DE-016962

Published in the USA, August 10, 2026
5994-9400EN